


ORIGINAL ARTICLE

SLC34A2 promotes cell proliferation by activating STX17-mediated autophagy in esophageal squamous cell carcinoma

Yi Xu¹ | Shiyu Duan² | Wen Ye¹ | Zhousan Zheng¹ | Jiaxing Zhang¹ | Ying Gao³ | Sheng Ye¹ 

¹Department of Oncology, The First Affiliated Hospital, Sun Yat-Sen University, Guangzhou, China

²Department of Pathology, Guangdong Provincial People's Hospital, Guangdong Academy of Medical Sciences, Guangzhou, China

³Department of Radiation Oncology, The First Affiliated Hospital, Sun Yat-Sen University, Guangzhou, China

Correspondence

Ying Gao, Department of Radiation Oncology, The First Affiliated Hospital, Sun Yat-Sen University, Guangzhou, China.
Email: gaoy325@mail.sysu.edu.cn

Sheng Ye, Department of Oncology, The First Affiliated Hospital, Sun Yat-Sen University, No. 58, Zhongshan 2 Road, 510080 Guangzhou, China.
Email: yesheng2@mail.sysu.edu.cn

Funding information

National Natural Science Foundation of China, Grant/Award Number: 81772513

Abstract

Background: Solute carrier family 34 member 2 (SLC34A2) has been implicated in the development of various malignancies. However, the clinical significance and underlying molecular mechanisms of SLC34A2 in esophageal squamous cell carcinoma (ESCC) remain elusive.

Methods: Western blotting, quantitative real-time PCR and immunohistochemistry were utilized to evaluate the expression levels of SLC34A2 mRNA/protein in ESCC cell lines or tissues. Kaplan–Meier curves were employed for survival analysis. CCK-8, colony formation, EdU and xenograft tumor model assays were conducted to determine the impact of SLC34A2 on ESCC cell proliferation. Cell cycle was examined using flow cytometry. RNA-sequencing and enrichment analysis were carried out to explore the potential signaling pathways. The autophagic flux was evaluated by western blotting, mRFP-GFP-LC3 reporter system and transmission electron microscopy. Immunoprecipitation and mass spectrometry were utilized for identification of potential SLC34A2-interacting proteins. Cycloheximide (CHX) chase and ubiquitination assays were conducted to test the protein stability.

Results: The expression of SLC34A2 was significantly upregulated in ESCC and correlated with unfavorable clinicopathologic characteristics particularly the Ki-67 labeling index and poor prognosis of ESCC patients. Overexpression of SLC34A2 promoted ESCC cell proliferation, while silencing SLC34A2 had the opposite effect. Moreover, SLC34A2 induced autophagy to promote ESCC cell proliferation, whereas inhibition of autophagy suppressed the proliferation of ESCC cells. Further studies showed that SLC34A2 interacted with an autophagy-related protein STX17 to promote autophagy and proliferation of ESCC cells by inhibiting the ubiquitination and degradation of STX17.

Conclusions: These findings indicate that SLC34A2 may serve as a prognostic biomarker for ESCC.

KEYWORDS

autophagy, ESCC, proliferation, SLC34A2, STX17

INTRODUCTION

Esophageal cancer is the eighth most common cancer and sixth leading cause of cancer-related mortality worldwide.^{1,2}

Esophageal squamous cell carcinoma (ESCC) is the predominant histological subtype of esophageal cancer in China. Despite advances in current therapeutic modalities, such as surgery, radiotherapy, chemotherapy and immunotherapy, the prognosis for ESCC patients remains unsatisfactory, with a five-year survival rate below 20%.¹ Therefore, it is

Yi Xu, Shiyu Duan and Wen Ye contributed equally to the study.

This is an open access article under the terms of the [Creative Commons Attribution-NonCommercial-NoDerivs](https://creativecommons.org/licenses/by-nc-nd/4.0/) License, which permits use and distribution in any medium, provided the original work is properly cited, the use is non-commercial and no modifications or adaptations are made.

© 2024 The Authors. *Thoracic Cancer* published by John Wiley & Sons Australia, Ltd.

imperative that the molecular mechanism of esophageal cancer development/progression is comprehensively investigated and elucidated in order to identify pivotal targets for effective ESCC treatment.

NaPi-2b (SLC34A2) is a transporter of sodium-dependent inorganic phosphate (Pi), maintaining optimal levels of inorganic phosphorus ion in various organs^{3,4} and multiple lumen fluids.⁵ SLC34A2 is predominantly expressed in the small intestine and type II alveolar cells (AT-II).⁶ Accumulating evidence suggests that SLC34A2 is abnormally expressed in different types of malignancies.⁷⁻⁹ Wang et al. found that SLC34A2 exerted suppressive effects on the proliferative, invasive and migrative behaviors of NSCLC cells.¹⁰ Another study revealed that knockdown of SLC34A2 inhibited cell growth via the PTEN/AKT/FOXO3a pathway in papillary thyroid carcinoma.¹¹ Moreover, a significant association was observed between elevated expression of SLC34A2 with the colorectal cancer (CRC) development, as well as unfavorable prognosis of CRC patients.⁸ Rearrangements of chromosomes, such as SLC34A2-ROS1 fusion, were detected in gastric and non-small cell lung cancers, resulting in the formation of hybrid proteins comprising both SLC34A2 and ROS1.^{12,13} To date, however, the precise molecular mechanisms underlying the role of SLC34A2 in ESCC remains poorly understood.

It is well established that autophagy refers to a cellular degradation and recycling process involved in the biogenesis of autophagosomes, fusion of autophagosomes with lysosomes, degradation in autolysosomes and utilization of degradation products.^{14,15} Numerous studies have demonstrated the involvement of autophagy in regulating tumorigenesis, invasion, metastasis, tumor immunity and chemoresistance.¹⁶⁻¹⁸ However, the roles of autophagy are complex and controversial in promoting cell survival or cell death depending on the cancer type, tumor stage and genetic context.¹⁹ Syntaxin 17 (STX17) is a major SNARE protein essential for mediating autophagosome-lysosome fusion.^{20,21} Inhibition of STX17 resulted in the accumulation of autophagosomes without degradation.²¹ Notably, STX17 has recently been reported to participate in autophagy initiation.²² By immunoprecipitation (IP) and mass spectrometry assays, STX17 was identified as an interacting protein of SLC34A2. However, the relationship between SLC34A2 and STX17 or autophagy in ESCC remain elusive.

Our studies revealed that SLC34A2 is markedly upregulated in ESCC and has a close association with unfavorable survival outcomes of ESCC patients. Overexpressing SLC34A2 exerted notable promoting effects on ESCC cell proliferation. Conversely, silencing SLC34A2 had the opposite results. Furthermore, SLC34A2 interacted with STX17 to activate autophagy by inhibiting the ubiquitination and degradation of STX17, thereby promoting cell proliferation. Collectively, our studies indicated that SLC34A2 could exert a crucial oncogenic role in ESCC and silencing SLC34A2 could be a therapeutic strategy for ESCC.

METHODS

Reagents

Dulbecco's modified Eagle medium (DMEM) and RPMI-1640 medium were purchased from Gibco (USA). Coomassie brilliant blue was sourced from Tiangen (China). The following antibodies were utilized: anti-SLC34A2 (66445S, 1:250 dilution for immunohistochemistry (IHC), 1:200 dilution for IF and 1:1000 dilution for WB, Cell Signaling Technology, USA), anti-Ki-67 (#9027S, 1:300 dilution for IHC, Cell Signaling Technology), anti-LC3B (#3868S, 1:1000 dilution for WB and 1:150 dilution for IHC, Cell Signaling Technology), anti-GAPDH (60004-1-Ig, 1:20000 dilution for WB, Proteintech Group, China), anti- α -tubulin (66031-1-Ig, 1:20000 dilution for WB, Proteintech Group), anti-TMEM106B (20995-1-AP, 1:1000 dilution for WB, Proteintech Group), anti-STX12 (14259-1-AP, 1:2000 dilution for WB, Proteintech Group), anti-p62/SQSTM1 (PM045, 1:1000 dilution for WB and 1:200 dilution for IHC, MBL Beijing Biotech Co.), syntaxin 17 (sc-518187, 1:1000 dilution for WB, 1:200 dilution for IF and 1:150 dilution for IHC, Santa Cruz Biotechnology).

Cell lines and cultures

Cell lines used in the study were obtained from Shanghai Cell Bank (China). Five human ESCC cell lines, namely KYSE70, KYSE140, KYSE410, KYSE520 and TE-1, were cultured in a RPMI 1640 medium with 10% fetal bovine serum (FBS) supplement. The normal esophageal epithelial cell line (NE-1) and retroviral packaging cell line (293 T) were cultured in a DMEM medium along with 10% FBS supplement. All cell lines were kept in a humidified incubator at 37°C with 5% CO₂.

Patient samples

Six pairs of fresh ESCC tissues and matched adjacent normal tissues were obtained from the First Affiliated Hospital, Sun Yat-Sen University in 2016. Paraffin-embedded tumor tissues were procured from 166 patients who had been diagnosed with ESCC and subsequently underwent surgical resection during the period between November 2007 and December 2008 at the First Affiliated Hospital of Sun Yat-sen University. They did not undergo any antitumor treatments prior to the surgical intervention. The clinicopathological staging was confirmed based on the seventh edition of the American Joint Committee on Cancer Tumor-Nodes-Metastasis (TNM) staging system. Detailed clinicopathological features of ESCC patients were described in Table 1. Ethical approval from the Medical Ethics Committee has been granted by the First Affiliated Hospital of Sun Yat-sen University (approval no. [2022]548) and informed consent was obtained from all patients.

TABLE 1 The relationship between SLC34A2 expression and clinicopathological features in ESCC patients.

Variable	All cases	Low SLC34A2 expression	High SLC34A2 expression	χ^2	p-value
	N = 166 (%)	N = 66 (%)	N = 100 (%)		
Age (years)				0.004	0.951
≤60	86 (51.8)	34 (39.5)	52 (60.5)		
>60	80 (48.2)	32 (40.0)	48 (60.0)		
Gender				0.175	0.676
Female	38 (22.9)	14 (36.8)	24 (63.2)		
Male	128 (77.1)	52 (40.6)	76 (59.4)		
Tumor recurrence				7.305	0.007*
No	67 (40.4)	35 (52.2)	32 (47.8)		
Yes	99 (59.6)	31 (31.3)	68 (68.7)		
Tumor size (cm)				0.489	0.484
≤3	81 (48.8)	30 (37.0)	51 (63.0)		
>3	85 (51.2)	36 (42.4)	49 (57.6)		
Tumor site				0.010	0.995
Upper segmental esophageal cancer	13 (7.8)	5 (38.5)	8 (61.5)		
Middle segmental esophageal cancer	103 (62.1)	41 (39.8)	62 (60.2)		
Lower segmental esophageal cancer	50 (30.1)	20 (40.0)	30 (60.0)		
T stage				6.925	0.008*
T1–T2	40 (24.1)	23 (57.5)	17 (42.5)		
T3–T4	126 (75.9)	43 (34.1)	83 (65.9)		
N stage				8.886	0.003*
N0	82 (49.4)	42 (51.2)	40 (48.8)		
N1–N2	84 (51.6)	24 (28.6)	60 (71.4)		
TNM stage				7.505	0.006*
I + II	89 (53.6)	44 (49.4)	45 (50.6)		
III	77 (46.4)	22 (28.6)	55 (71.4)		
Histological grade				6.591	0.037*
Well (I)	34 (20.5)	20 (58.8)	14 (41.2)		
Moderate (II)	80 (48.2)	27 (33.8)	53 (66.3)		
Poor (III)	52 (31.3)	19 (36.5)	33 (63.5)		
Ki-67 labeling index				10.483	0.001*
High (≥45%)	81	22 (27.2)	59 (72.8)		
Low-moderate (<45%)	85	44 (51.8)	41 (48.2)		

Abbreviations: ESCC, esophageal squamous cell carcinoma; SLC34A2, solute carrier family 34 member 2.

* $p < 0.05$.

Western blotting (WB)

To obtain the total cell lysates, we utilized a radioimmunoprecipitation (RIPA) buffer which was supplemented with phosphatase and proteinase inhibitor cocktails. After quantifying the total protein concentration of lysates, the protein samples were separated by 12% SDS-PAGE and then transferred onto polyvinylidene fluoride (PVDF) membranes. After that, a blocking step using 5% skim milk prior to incubation with primary antibodies was performed. Subsequently, the membranes were incubated with secondary antibodies. To detect the immunoreactivity of the membranes, we utilized an electrochemiluminescence system from Thermo Fisher Scientific and BioRad Image Laboratory.

RNA isolation and qRT-PCR

Total RNA extraction from ESCC cell lines was carried out using TRizol reagent (Invitrogen). To perform quantitative real-time polymerase chain reaction (qRT-PCR), we adopted the 2× Color SYBR Green qPCR Master Mix (EZBioscience) on a QuantStudio 5 RT-PCR System (Thermo Fisher Scientific). The primer sequences (Tsingke Biotechnology Co.) used in the study were as follows: SLC34A2 forward primer, 5'-CTCTGCCAAG-TATCGCTGGT-3', SLC34A2 reverse primer, 5'-TGGAGTTTCTTCGGCAGGAC-3', STX17 forward primer, 5'-CATGACTGTTGGTGGAGCATTTC-3', STX17 reverse primer, 5'-GCTTCTAAGGTTCCACGATTC-3', β -actin

forward primer, 5'-CCTTCCTGGGCATGGAGTC-3', β -actin reverse primer, 5'-TGATCTTCATTGTGCTG GGTG-3'. β -actin served as an internal control. The relative expression of SLC34A2 and STX17 was calculated using the $2^{-\Delta\Delta C_t}$ method.

Immunohistochemistry (IHC)

Briefly, paraffin-embedded samples were orderly deparaffinized, rehydrated and boiled in citrate buffer (pH = 6.0) for antigen retrieval. Subsequently, these sections were exposed to hydrogen peroxide and treated with primary antibodies overnight, followed by incubation with secondary antibodies for 1 h and visualization with diaminobenzidine (DAB) (ZSGB-BIO). To counterstain the nuclei, Mayer's hematoxylin was utilized.

Two pathologists scored the slides separately by a double-blind approach. IHC scores were calculated by multiplying the staining intensity scores and the proportion scores of positive cells. Specifically, staining intensity was graded on the basis of the following criteria: 0 (negative, no staining), 1 (weak, light-yellow), 2 (moderate, yellow-brown), and 3 (strong, brown) staining. The proportion of positively stained tumor cells was evaluated as follows: 0 denoted an absence of staining in any cell; 1 represented staining in 1%–10% of tumor cells; 2 indicated staining in 11%–50% of tumor cells; 3 represented staining in 51%–80% of tumor cells, and 4 indicated staining in 81%–100% of tumor cells. To perform statistical analysis, we divided the cohort of 166 patients with ESCC into two groups: low SLC34A2 expression group (“–” [0 score] and “+” [1–4 scores]) and high SLC34A2 expression group (“++” [5–8 scores] and “+++” [9–12 scores]).

Plasmid constructs and transfection

To produce the SLC34A2 expression vector, we cloned the amplified coding sequences of SLC34A2 into a pLVX-puro vector. Specifically, we conducted PCR amplification of the full-length human SLC34A2 complementary DNA and then inserted it into the pLVX-puro expression vector (Tsingke Biotechnology Corporation). To generate lentiviruses, we transfected 293 T cells with target plasmids and packaging plasmids mix (Tsingke Biotechnology Corporation). Then, KYSE520 cells were infected with these harvested lentiviruses and selected in puromycin (MCE). Control cells were generated by transfection with an empty vector.

Construction of the recombinant lentiviral vector or siRNAs

The shRNAs targeting SLC34A2 (GenBank accession no. NM_006424.3; shSLC34A2-1#, CCGGGCCAACAT TGGAACGTCAATCCTCGAGGATTGACGT-TCCAAT GTGGCTTTTTT; shSLC34A2-2#, CCGGCCAGCA

TATCTTTGTGA-ATTTCTCGAGAAATTCACAAAGA TATGCTGGTTTTTT) were designed and constructed by Tsingke Biotechnology Corporation (China) using the pLKO.1-Puro-TRC vector. A negative control vector with a scrambled sequence (shSLC34A2-scramble) was purchased from Tsingke Biotechnology Corporation. We infected KYSE410 and TE-1 cell lines with retroviruses that carried pLKO.1-Puro-TRC-SLC34A2-shRNA due to the high expression of SLC34A2. Stable cells were selected using puromycin. The siRNAs targeting STX17 (NCBI Gene: 55014; siSTX17-2#, 5'-GGGACAAGTTGCATGAAGA-3'; siSTX17-3#, 5'-CCGAAAGGATGACCTAGTA-3') and a negative control were designed and constructed by RiboBio (China).

CCK-8 and colony formation assays

Cells (1.5×10^3 cells/well) were seeded into 96-well plates. The viability of cells was measured every 24 h by using a cell counting kit-8 (CCK-8 kit: APEX BIO, USA) according to the manufacturer's protocol.

For assessing the colony forming ability, we seeded 300 infected cells into a six-well plate and they were cultured at standard conditions for 10–14 days. After the incubation period, we employed a standardized procedure in which we initially utilized a solution of methanol to fix the cells. Following this, crystal violet staining solution (0.1%) was used to visualize the colonies. The counting and photography of the colonies were conducted thereafter.

5-ethynyl-2'-deoxyuridine (EdU) assay

To accurately assess the cell proliferation ability, we utilized a highly specific and sensitive assay involving the BeyoClick EdU cell proliferation kit (Beyotime). Confocal plates were utilized to seed cells at a density of 1×10^5 cells per well. Cells were incubated with an EdU buffer at a concentration of 10 μ M for a couple of hours at 37°C, and then fixed by a 4% formaldehyde solution for 0.5 h, followed by permeabilization using a 0.1% Triton X-100 solution for 20 min. After introducing the EdU solution to the culture, the nuclei of cells were stained with Hoechst 33342 and subsequently visualized using a fluorescence microscope.

Flow cytometry

Cells were seeded into six-well plates and allowed to grow until they reached approximately 80% confluence. A single cell was produced using trypsin without EDTA, fixed in ice-cold 75% ethanol overnight for 12 h and then incubated with 500 μ L of PI/RNase staining buffer (4A Biotech Co., Ltd) for 15 min in darkness at RT. Analysis of the samples was performed using Beckman flow cytometry (CytoFLEX).

Xenograft tumor model assay

BALB/c female nude mice (4 weeks old) were randomized into four groups. An equivalent number of TE-1 shSLC34A2-1/scramble cells and KYSE520-SLC34A2/Control cells (3×10^6 cells/mL) were resuspended in phosphate buffered saline (PBS) and injected into the dorsal flank of each nude mouse. The formula utilized to determine tumor volume was multiplying the longest diameter of the tumor by the square of the shortest diameter, and then dividing that result by two. Mice were followed up every 3 days to measure tumor sizes. After 22 days, ethical euthanasia was performed on all mice, and the tumors were meticulously removed, weighed, and photographed to obtain detailed morphological information. Animal experiments were approved by the Medical Ethics Committee of Sun Yat-sen University (approval no. SYSU-IACUC-2022-001771).

Immunoprecipitation (IP) assay

Cell extracts were resuspended, then lysed in precooled IP buffer (Solarbio, China) for 20 min and centrifuged for 15 min. Protein A/G magnetic beads (Bimake, China) or anti-HA magnetic beads (MCE, USA) were added into collected cell lysate and incubated for 8–12 h at 4°C. After that, the above-mentioned complexes were supplemented with antibody (5 µg) and allowed to incubate for 1–2 h at room temperature. Finally, the immunoprecipitated proteins were eluted by boiling in SDS loading buffer (2×) for WB analysis.

Immunofluorescence staining

ESCC cells (5×10^3 cells/mL) were seeded into confocal plates and cultured for 24 h. Before being permeabilized with Triton X-100 (0.1%) for 10 min, the cells were fixed with 4% paraformaldehyde (PFA) for 0.5 h. They were subsequently blocked with bovine serum albumin (BSA) (5%) for 1 h at RT. The cells were then exposed to the primary antibody overnight at 4°C, followed by incubation with fluorescence-labeled secondary antibodies incubation for 1 h the next day and stained using 4',6-diamidino-2-phenylindole (DAPI; Solarbio) for 10 min. Finally, immunofluorescence was observed under an inverted laser confocal microscope (FV3000, Olympus).

Additionally, ESCC cells were transfected with mRFP-GFP-LC3B lentivirus (Hanbio Co. Ltd, China), fixed with 4% formaldehyde and stained with DAPI. After that, images were directly captured via a confocal microscope. The quantification of colored puncta per cell, a measure of autophagy, was performed in a blinded manner by an independent observer.

Transmission electron microscopy (TEM)

Cell samples were first fixed with 2.5% glutaraldehyde (Servicebio) and then post-fixed with osmium tetroxide

(1%). After thrice washing with PBS, the samples were dehydrated in a series of ethanol (50%–100%) and ultrathin sections were obtained. Finally, the sections were observed under a transmission electron microscope (JEM-1200EX, JEOL) after impregnation with uranyl acetate and lead citrate.

In vivo ubiquitination assay

Cells were cultured in 6-cm plates and transfected with 2 µg of pcDNA3-3 × His-Ub (Genecreate, China) for 8 h. After 48 h, the cells underwent treatment with 10 µM of MG132 (MCE) for 8 h and were suspended in a volume of 1 mL of PBS. Then, 100 µL of the cell suspension was mixed with SDS loading buffer (Leagene) and boiled to perform immunoblot analysis with STX17 and GAPDH antibodies. The remaining cells were lysed using Buffer C. Next, the lysates were sonicated and combined with 30 µL of Ni-NTA (His-tag Affinity) magnetic beads (Thermo Fisher Scientific) at RT for 4 h. Subsequently, the beads were orderly washed twice with buffer C, buffer D and buffer E. The configuration method of the above-mentioned reagents has been previously described.²³ Then bound proteins were efficiently eluted by boiling in a 2 × SDS loading buffer. After that, the samples were subjected to immunoblot analysis with an anti-STX17 monoclonal antibody.

Statistical analysis

All cellular experiments were carefully repeated at least thrice. The resulting data were meticulously analyzed using SPSS 19.0 and GraphPad Prism 8.0 software. The statistical analysis involved calculating the mean ± standard deviation ($X \pm SD$) of the data. To evaluate differences between SLC34A2 expression and clinicopathological variables, the Chi-square test or the Fisher's exact test was utilized. The Kaplan–Meier curves and log-rank test were employed for survival analysis. Differences between a couple of groups were compared using paired or unpaired two-tailed student's *t*-test. When multiple groups were involved in comparisons, one-way analysis of variance (ANOVA) was utilized. A *p*-value of less than 0.05 was considered statistically significant.

RESULTS

SLC34A2 is significantly upregulated in ESCC and closely correlates with unfavorable prognosis of ESCC patients

WB and qRT-PCR were conducted to examine the protein and mRNA levels of SLC34A2 in ESCC cells and tissues. As shown in Figure 1a,b, six ESCC tissues exhibited higher protein and mRNA levels of SLC34A2 than those in adjacent noncancerous tissues. Furthermore, five ESCC cell

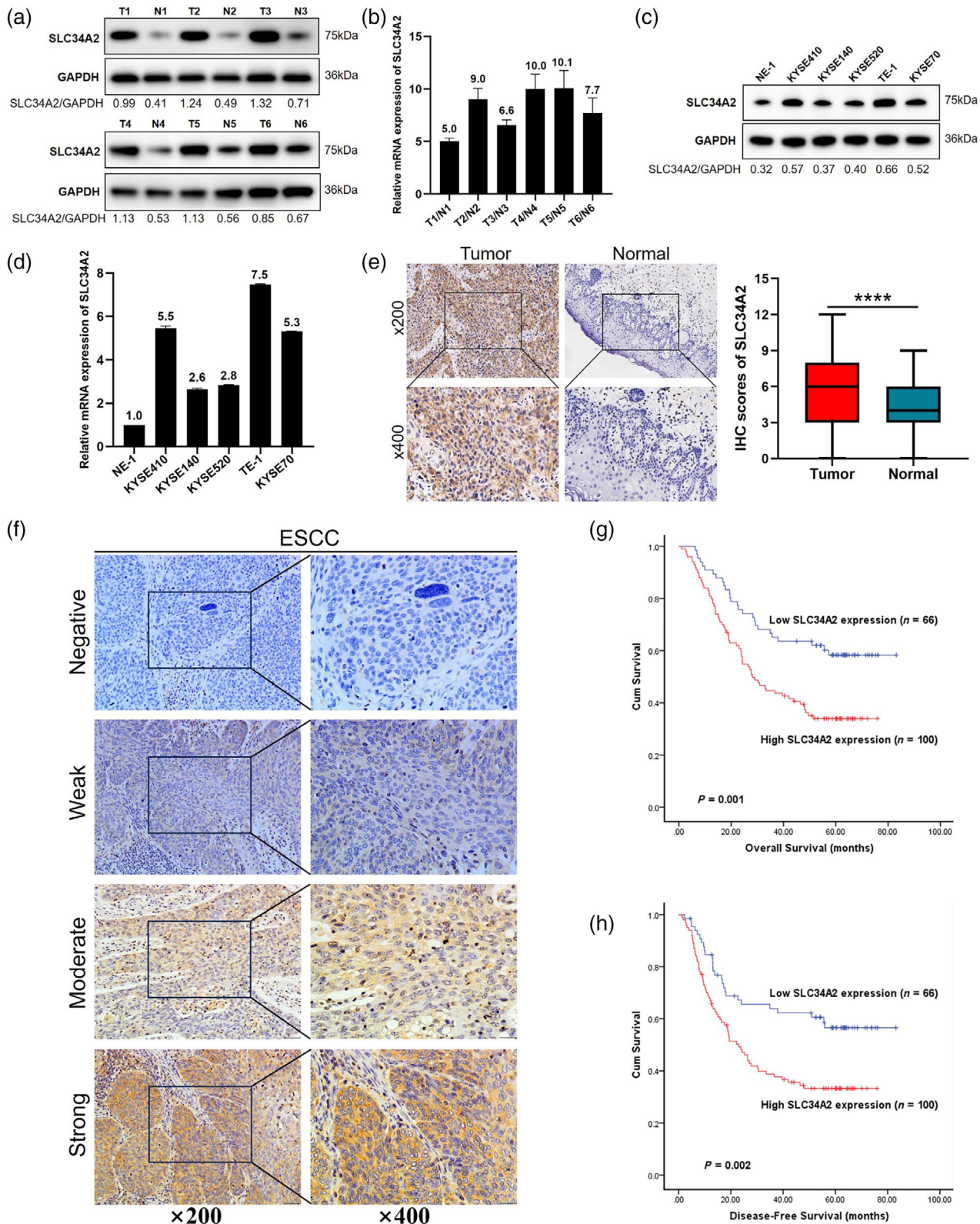


FIGURE 1 Solute carrier family 34 member 2 (SLC34A2) is significantly upregulated in esophageal squamous cell carcinoma (ESCC) and associated with an unfavorable prognosis for ESCC patients. (a, b) The expression levels of SLC34A2 protein and mRNA in six pairs of fresh ESCC tissues and matched normal tissues were measured using western blot (WB) and quantitative reverse transcription polymerase chain reaction (qRT-PCR). (c, d) The expression levels of SLC34A2 protein and mRNA in NE-1 and five ESCC cell lines were evaluated using WB and qRT-PCR. (e) Representative immunohistochemistry (IHC) staining images of SLC34A2 in 166 paired human ESCC tissues and adjacent normal tissues. (f) Representative images of negative, weak, moderate and strong SLC34A2 IHC staining in ESCC tissues are shown. (g, h) Kaplan-Meier curve was deployed to assess overall survival (OS) and disease-free survival (DFS) rates for ESCC patients with low or high SLC34A2 expression. The grayscale value of the target protein in the WB was quantified using ImageJ software and normalized to glyceraldehyde 3-phosphate dehydrogenase (GAPDH). **** $p < 0.0001$.

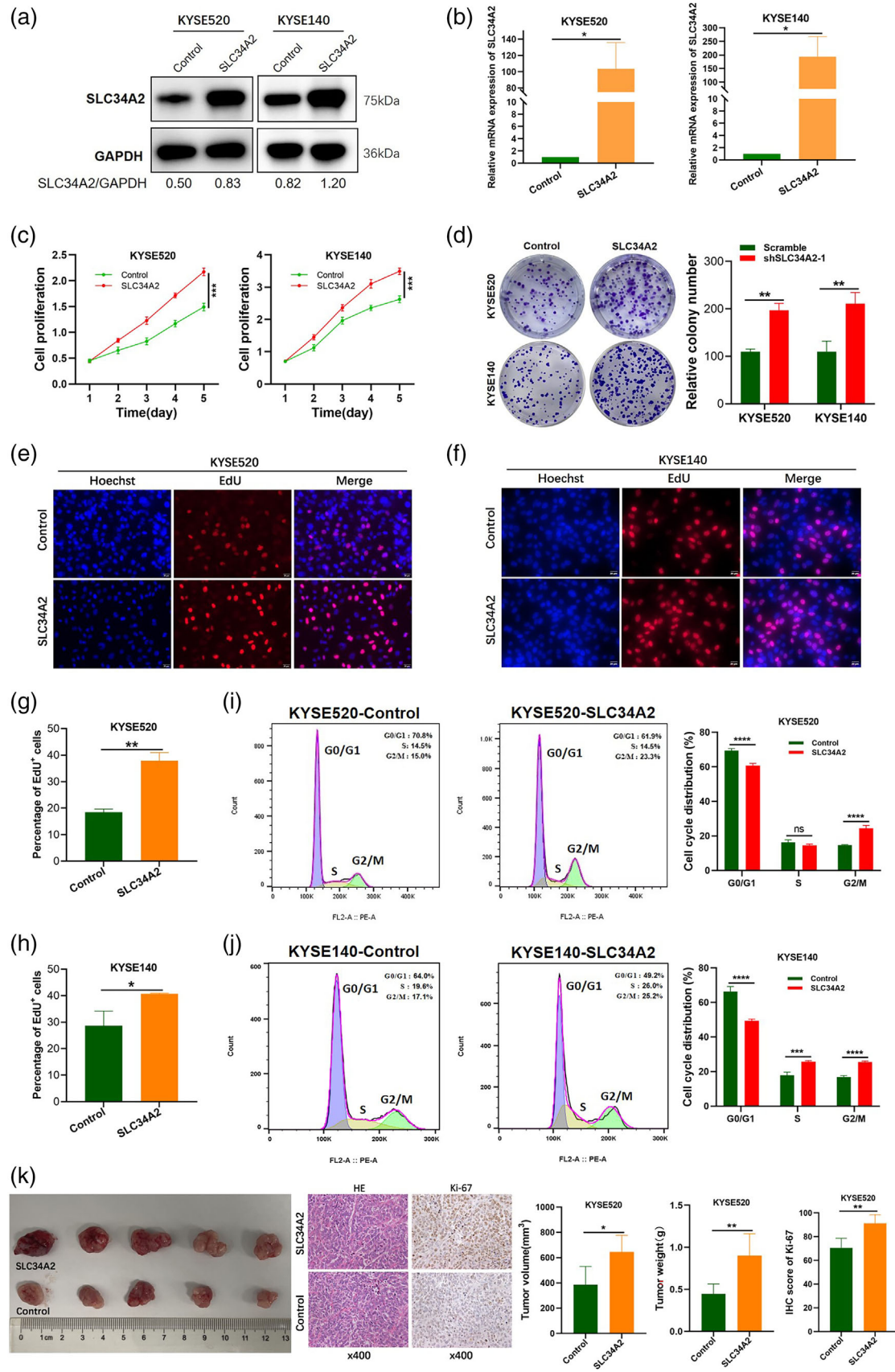


FIGURE 2 Legend on next page.

lines showed elevated protein and mRNA levels of SLC34A2 compared to NE-1 (Figure 1c,d). IHC analysis further showed that primary ESCC tissues displayed upregulated expression of SLC34A2 relative to matched normal tissues (Figure 1e), with positive staining mainly observed in the cytoplasm of tumor cells (Figure 1f). Notably, high expression of SLC34A2 was significantly associated with unfavorable characteristics such as tumor recurrence ($p = 0.007$), T stage ($p = 0.008$), N stage ($p = 0.003$), TNM stage ($p = 0.006$), histological grade ($p = 0.037$) and Ki-67 labeling index ($p = 0.001$) (Table 1). Moreover, the Kaplan–Meier curves revealed that those ESCC patients with high SLC34A2 expression had shorter overall survival (OS, $p = 0.001$, Figure 1g) and disease-free survival (DFS, $p = 0.002$, Figure 1h) than those exhibiting low SLC34A2 expression. Collectively, these results reveal that SLC34A2 is overexpressed in ESCC and high SLC34A2 expression is closely correlated with poor prognosis of ESCC patients.

Overexpression of SLC34A2 promotes ESCC cell proliferation in vitro and in vivo

Based on the close relationship between elevated SLC34A2 expression and a high Ki-67 labeling index, we further explored the effects of SLC34A2 on ESCC cell proliferation. Initially, we overexpressed SLC34A2 in KYSE520 and KYSE140 cells by lentivirus transfection and assessed the transfection efficacy using WB and qRT-PCR (Figure 2a,b). Subsequently, CCK-8, colony formation and EdU assays revealed that upregulation of SLC34A2 significantly promoted the proliferation of ESCC cells (Figure 2c–h). What's more, analysis of cell cycle distribution revealed that overexpression of SLC34A2 led to a remarkable decrease in the proportion of G0/G1 phase cells while simultaneously increasing the proportion of G2/M phase cells (Figure 2i,j), indicating that SLC34A2 overexpression accelerated cell cycle progression. The xenograft tumor model further suggested that elevated expression of SLC34A2 accelerated the growth of ESCC cells in vivo (Figure 2k). Additionally, the immunohistochemical staining exhibited a higher Ki-67 proliferation index in the SLC34A2-overexpressed tumors than that in the control tumors (Figure 2k). Therefore, these findings confirm that SLC34A2 upregulation promotes the growth of ESCC cells both in vitro and in vivo.

Knockdown of SLC34A2 inhibits ESCC cell proliferation in vitro and in vivo

To investigate the impact of SLC34A2 knockdown on cell proliferation, we employed a lentiviral shRNA technique to establish two ESCC cell lines with stable knockdown of SLC34A2. The efficacy of knockdown was evaluated by WB and qRT-PCR (Figure 3a,b). As depicted in Figure 3c–e, downregulation of SLC34A2 significantly inhibited ESCC cell proliferation in vitro. Furthermore, cell cycle distribution analysis suggested that silencing SLC34A2 contributed to a notable increase in the proportion of G0/G1 phase cells and a corresponding decrease in the number of G2/M phase cells (Figure 3f), indicating that SLC34A2 downregulation led to G0/G1 cell cycle arrest.

Moreover, our findings demonstrated that knockdown of SLC34A2 effectively impeded the growth of ESCC cells in vivo (Figure 3g). Immunohistochemical staining exhibited a substantially lower Ki-67 proliferation index in SLC34A2-decreased tumors compared to control tumors (Figure 3g). Collectively, these data provide compelling evidence for the inhibitory effect of SLC34A2 knockdown on ESCC cell proliferation in vitro and in vivo.

SLC34A2 promotes ESCC cell proliferation by inducing autophagy

To elucidate the possible mechanisms underlying SLC34A2-mediated cell proliferation, we performed RNA-sequencing on SLC34A2-overexpressed cells of KYSE520 and control cells. Gene set enrichment analysis (GSEA) revealed proliferation-associated signaling pathways among the enriched pathways as shown in Figure 4a. Additionally, it was discovered that gene sets of AUTOPHAGOSOME and AUTOPHAGOSOME_MEMBRANE were positively correlated with high SLC34A2 expression in ESCC cells (Figure 4b,c). A growing body of evidence indicate that activation of autophagy can promote ESCC cell proliferation^{24,25} by meeting high metabolic and energetic demands of malignant cells. Thus, it was attempted to investigate whether SLC34A2-mediated cell proliferation was dependent on autophagy. Firstly, autophagy-related proteins LC3B and P62 were evaluated by WB analysis. Notably, decreased P62 expression and increased LC3B expression were detected in SLC34A2-upregulated cells, while decreased LC3B expression and increased P62 expression were observed in SLC34A2-downregulated cells after a 2-h

FIGURE 2 Overexpression of solute carrier family 34 member 2 (SLC34A2) promotes esophageal squamous cell carcinoma (ESCC) cell proliferation in vitro and in vivo. (a, b) Western blot (WB) and quantitative reverse transcription polymerase chain reaction (qRT-PCR) were performed to analyze the SLC34A2 protein and mRNA levels in stably SLC34A2-overexpressed KYSE520 and KYSE140 cells. (c–h) Cell counting kit-8 (CCK-8) (c), colony formation (d) and 5-ethynyl-2'-deoxyuridine (EdU) (e–h) assays were conducted to measure the proliferative capacity of SLC34A2-overexpressed ESCC cells. Scale bar, 20 μm . (i, j) Cell cycle distribution in SLC34A2-overexpressed ESCC cell was assessed by flow cytometry. (k) The xenograft tumor photographs of nude mice injected with KYSE520/SLC34A2 cells or KYSE520/control cells ($n = 5$). The tumor volume (mm^3) and weight (g) were measured. HE and Ki-67 staining of xenograft tumors were evaluated (magnification, $\times 400$). The grayscale value of the target protein in the WB was quantified using ImageJ software and normalized to GAPDH. ns, not significant; * $p < 0.05$; ** $p < 0.01$; *** $p < 0.001$; **** $p < 0.0001$.

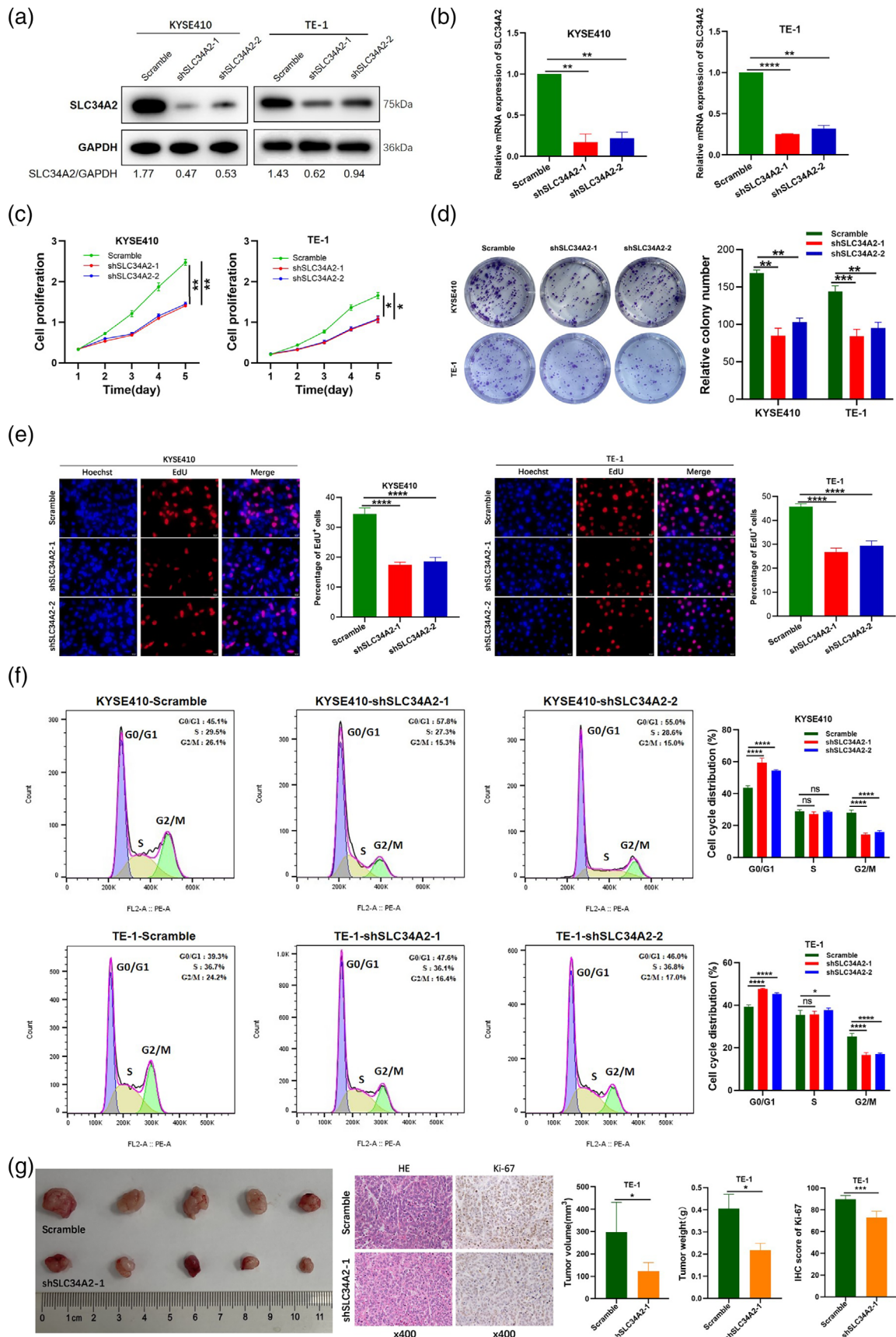


FIGURE 3 Legend on next page.

incubation in Earle's balanced salt solution (EBSS) (Figure 4d). The mRFP-GFP-LC3 reporter system was utilized to assess autophagic flux, in which yellow (mRFP+ and GFP+) dots represented autophagosomes and red (mRFP+ and GFP-) dots indicated autolysosomes. After 2 h of EBSS treatment, versus control cells, a notable increase was identified in the quantity of autophagosomes and autolysosomes in SLC34A2-overexpressed cells, while autophagosomes and autolysosomes were reduced in SLC34A2-downregulated cells (Figure 4e). Furthermore, there was a remarkable increase in the number of autophagic vacuoles (AVs) after SLC34A2 upregulation (Figure 4f). The above-mentioned results suggest that SLC34A2 activate autophagy in ESCC.

To confirm the functional roles of SLC34A2-regulated autophagy in ESCC cell proliferation, we treated SLC34A2-overexpressed ESCC cells with an autophagy inhibitor bafilomycin A1 (BafA1, MCE, USA; final concentration: 50 nM; 24 h). Notably, the proproliferative effects of SLC34A2 overexpression were abrogated by BafA1 (Figure 4g,h). Conversely, the inhibitory effects on ESCC cell proliferation after SLC34A2 knockdown were reversed upon treatment with the autophagy stimulator rapamycin (RAPA, MCE, USA; final concentration: 100 nM; 24 h), as described in Figure 4i,j and Figure S1a,b. Taken together, there is evidence that SLC34A2 may promote ESCC cell proliferation by inducing autophagy.

Overexpression of SLC34A2 promotes ESCC cell proliferation and autophagy by upregulating STX17

We employed IP in conjunction with Coomassie brilliant blue staining and mass spectrometry to identify potential SLC34A2-interacting proteins (Figure 5a). The autophagy-related proteins among them were screened (Table S1) and the interaction between three top-ranking proteins and SLC34A2 was further tested by IP. The results showed that only STX17 protein interacted with SLC34A2 (Figure 5b). Subsequently, we revealed that endogenous binding could occur between SLC34A2 and STX17 in ESCC cells as evidenced by Co-IP and WB (Figure 5c). Additionally, immunofluorescence localization studies validated that SLC34A2 and STX17 were predominantly colocalized in the cytoplasm of ESCC cells, as illustrated in Figure S2. To figure out how SLC34A2 regulated STX17, we evaluated the STX17 protein and mRNA levels after SLC34A2

overexpression or knockdown. It was uncovered that overexpression of SLC34A2 contributed to upregulation of STX17 protein (Figure 5d), while no changes were identified in the mRNA level of STX17 (Figure S3), suggesting that SLC34A2 could regulate STX17 post-translationally.

To investigate the impact of STX17 on ESCC cell proliferation and autophagy, we knocked down STX17 expression in SLC34A2-overexpressed ESCC cells. By WB analysis, upregulated P62 expression and reduced LC3B expression were found after STX17 knockdown (Figure 5e). Moreover, the number of autophagosomes and autolysosomes was markedly decreased in STX17-silenced ESCC cells (Figure 5f), revealing that autophagy was blocked after downregulating STX17. Functionally, the pro-proliferative role of SLC34A2 overexpression was effectively reversed upon silencing STX17, as shown in Figure 5g-i. Furthermore, downregulated LC3B expression and upregulated P62 expression were detected by IHC in subcutaneous tumors after silencing STX17 (Figure S4). Taken together, these findings demonstrate that SLC34A2 overexpression promotes ESCC cell proliferation and autophagy by upregulating STX17 expression.

SLC34A2 inhibits the ubiquitination and degradation of STX17 by interacting with STX17

As it was observed that SLC34A2 affected the protein level rather than mRNA level of STX17, the cycloheximide (CHX) chase experiment was conducted to investigate the impact of SLC34A2 on the stability of STX17. Results demonstrated that SLC34A2 extended the half-life of STX17 protein (Figure 6a,b). Subsequently, *in vivo* ubiquitination assay was carried out to address how SLC34A2 affected STX17 protein stability in ESCC cells. After treatment with MG132, it was revealed that upregulation of SLC34A2 inhibited the ubiquitination of STX17 (Figure 6c), while knockdown of SLC34A2 promoted the ubiquitination of STX17 (Figure 6d). These findings suggest that SLC34A2 enhances STX17 protein stability by interacting with STX17.

DISCUSSION

Despite a growing body of evidence that highlights the potential involvement of SLC34A2 in tumor development and progression,^{10,26-28} the intricate molecular mechanisms

FIGURE 3 Knockdown of solute carrier family 34 member 2 (SLC34A2) inhibits esophageal squamous cell carcinoma (ESCC) cell proliferation *in vitro* and *in vivo*. (a, b) The protein and mRNA levels of SLC34A2 were analyzed using western blot (WB) and quantitative reverse transcription polymerase chain reaction (qRT-PCR) in SLC34A2-downregulated cells. (c-e) The proliferative ability of SLC34A2-downregulated ESCC cells were analyzed by cell counting kit-8 (CCK-8), colony formation and 5-ethynyl-2'-deoxyuridine (EdU) assays. Scale bar, 20 μ m. (f) Cell cycle distribution in SLC34A2-downregulated ESCC cells was assessed by flow cytometry. (g) The xenograft tumor photographs of nude mice injected with TE1/shSLC34A2-1 cells and TE-1/scramble cells ($n = 5$). The tumor volume (cm^3) and weight (g) were measured. HE and Ki-67 staining of xenograft tumors in each group were evaluated (magnification, $\times 400$). The grayscale value of the target protein in the WB was quantified using ImageJ software and normalized to glyceraldehyde 3-phosphate dehydrogenase (GAPDH). ns, not significant; * $p < 0.05$; ** $p < 0.01$; *** $p < 0.001$; **** $p < 0.0001$.

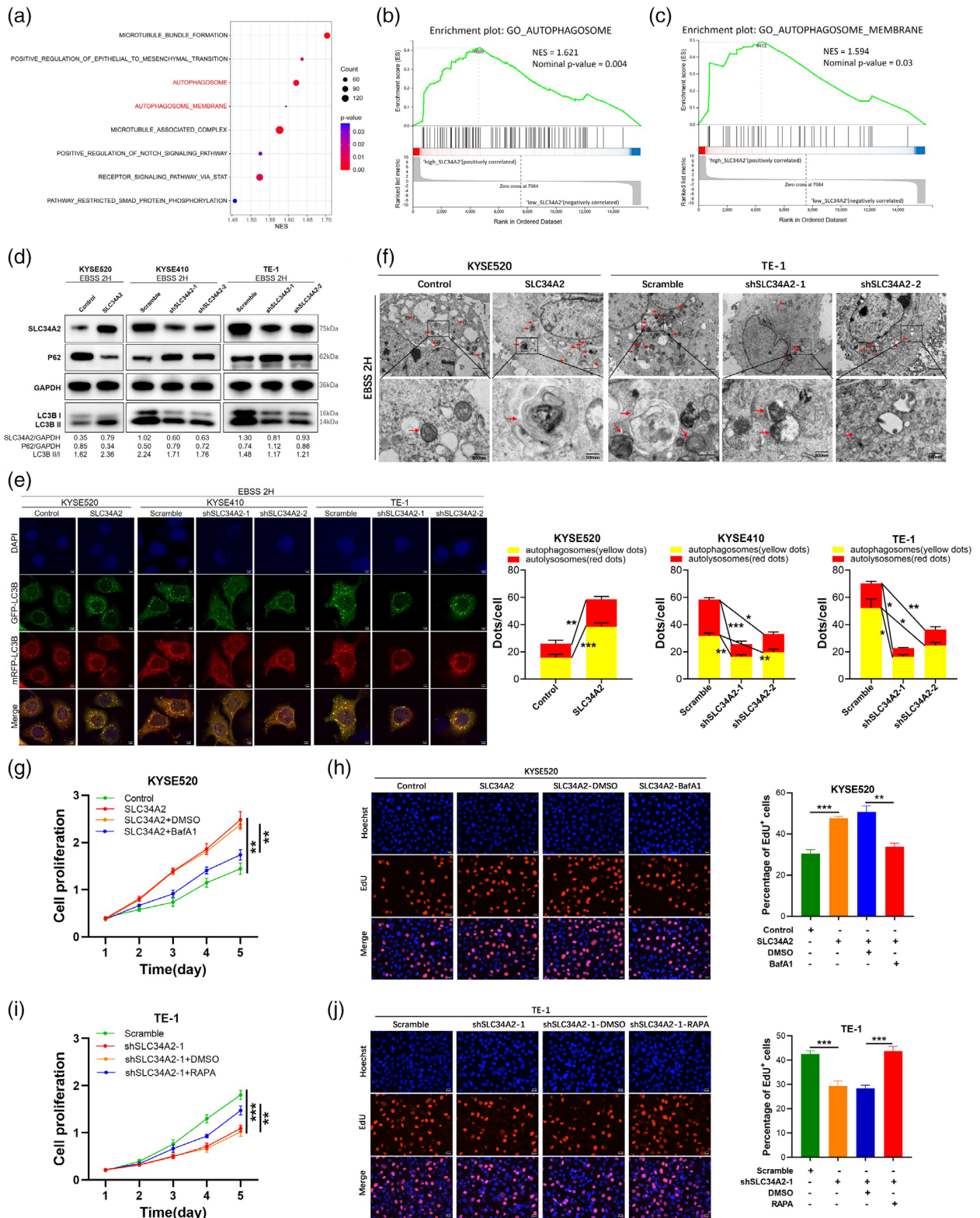


FIGURE 4 Solute carrier family 34 member 2 (SLC34A2) promotes esophageal squamous cell carcinoma (ESCC) cell proliferation by inducing autophagy. (a) The proliferation-associated signaling pathways among the enriched pathways were shown by gene set enrichment analysis (GSEA) based on RNA-sequencing data of SLC34A2-overexpressed cells. (b, c) Gene sets of autophagosome and autophagosome_membrane were positively correlated with high SLC34A2 expression in ESCC by GSEA. (d) Protein of LC3B and P62 were examined by western blot (WB) when SLC34A2-upregulated or SLC34A2-downregulated cells were cultured in Earle's balanced salt solution (EBSS) for 2 h. (e) SLC34A2-overexpressed/–downregulated cells were transfected with mRFP-GFP-LC3B lentiviruses and cultured for 48 h. After 2 h of EBSS treatment, green and red fluorescence were detected under laser confocal microscope. Scale bar, 5 μm. (f) Electron microscopy was conducted to visualize the ultrastructure of the ESCC cells after SLC34A2 overexpression or knockdown. Red arrows represent autophagic vacuoles (AVs). Magnification scale bar, 2 μm (upper) and 500 nm (lower). (g–j) Cell counting-kit 8 (CCK-8) and 5-ethynyl-2'-deoxyuridine (EdU) assays were carried out to detect the proliferative ability of ESCC cells by treatment with BafA1 or RAPA. The grayscale value of the target protein in the WB was quantified using ImageJ software and normalized to glyceraldehyde 3-phosphate dehydrogenase (GAPDH). Scale bar, 20 μm. * $p < 0.05$; ** $p < 0.01$; *** $p < 0.001$.

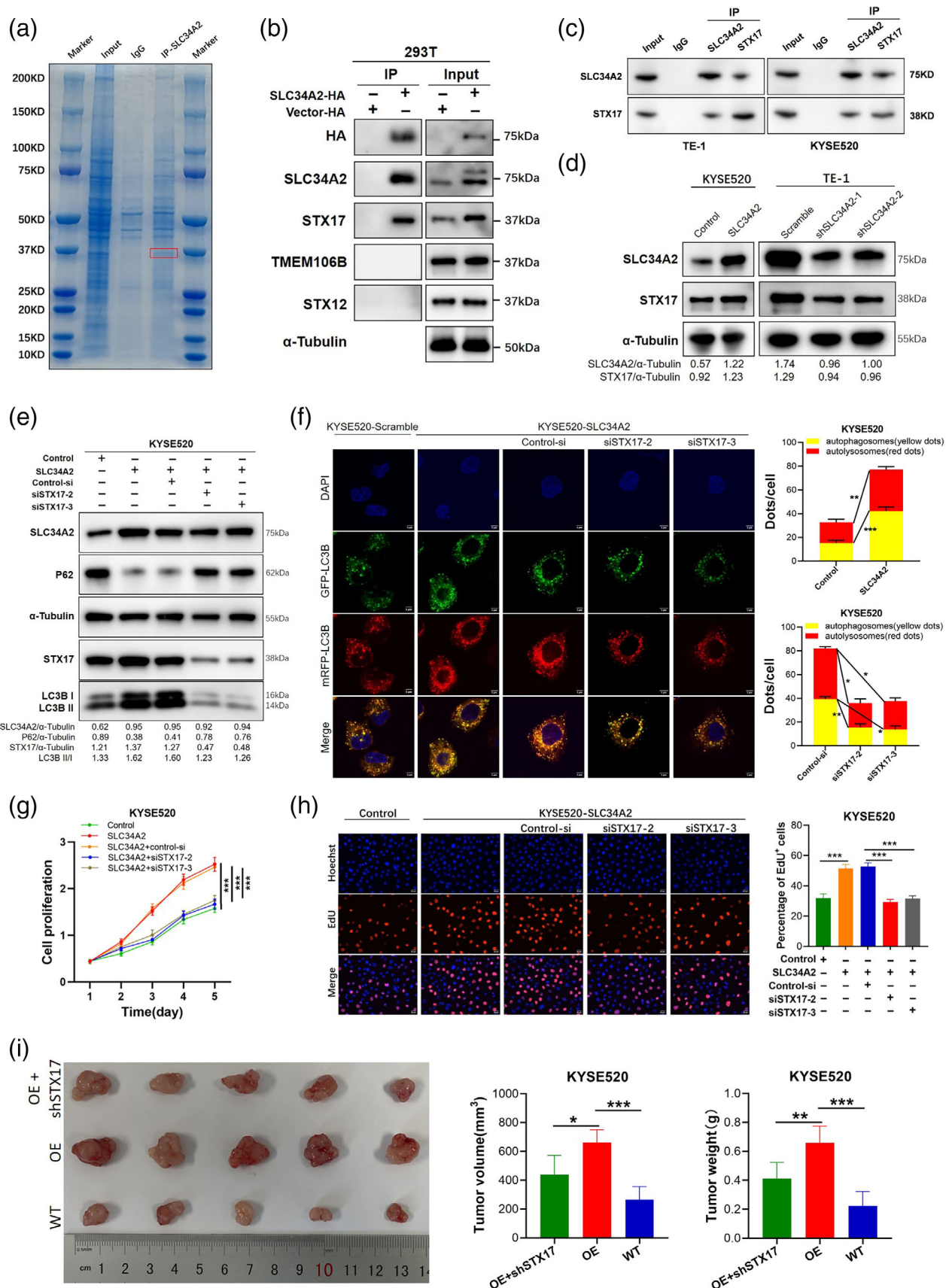


FIGURE 5 Legend on next page.

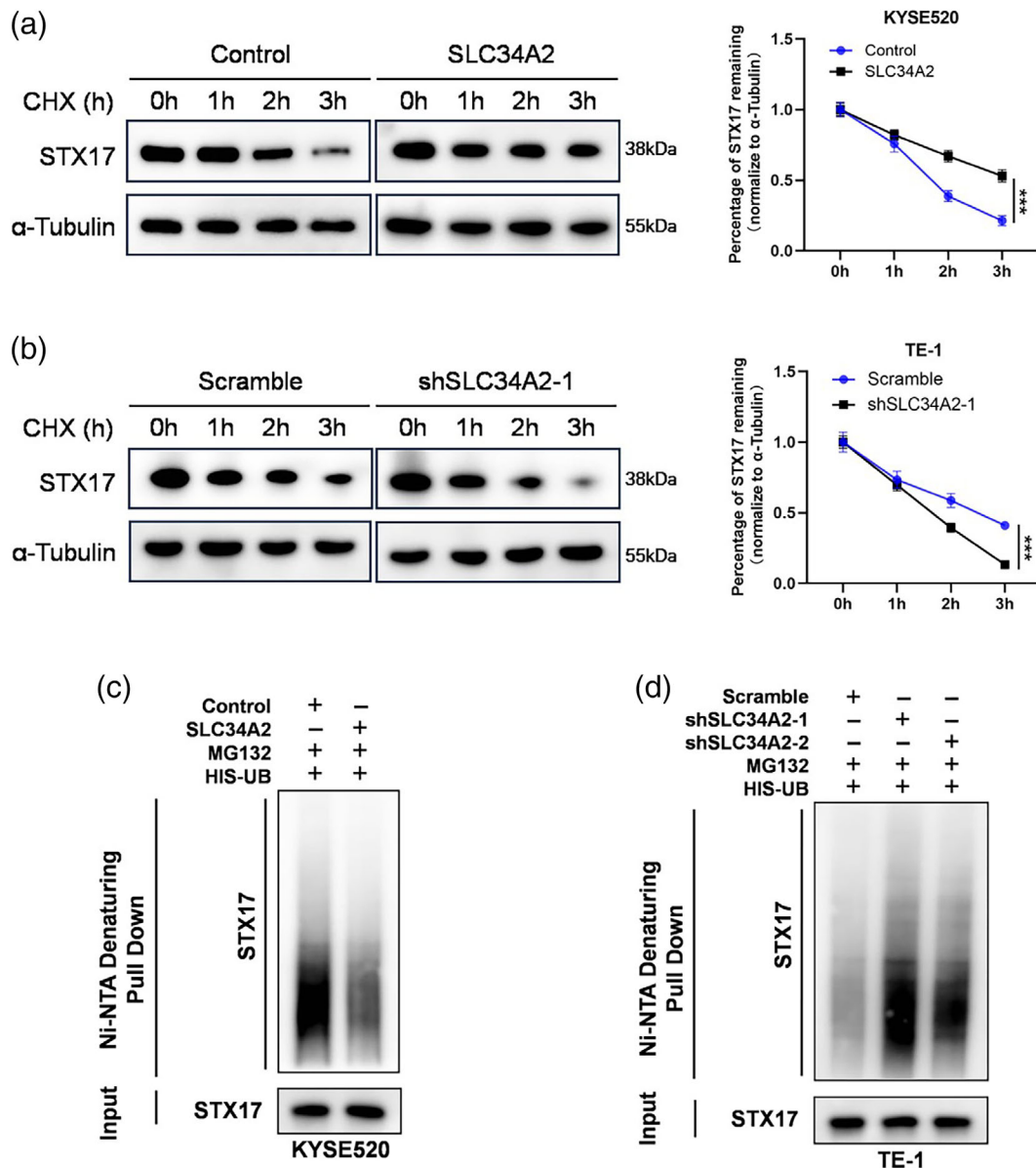


FIGURE 6 Solute carrier family 34 member 2 (SLC34A2) inhibits the ubiquitination and degradation of STX17. (a, b) SLC34A2-overexpressed/–silenced cells were treated with translational inhibitor cycloheximide (CHX, 100 μ mol/L) at various time points before being collected for western blot (WB). The expression levels of STX17 were normalized against loading control α -tubulin. (c, d) The stability of STX17 protein was evaluated by the ubiquitination assay in SLC34A2-overexpressed/–silenced cells after treatment with MG132. *** $p < 0.001$.

underlying this phenomenon remains limited. The present study indicated that SLC34A2 was highly expressed in ESCC cells and tissues. The data revealed a close relationship

between elevated SLC34A2 expression in ESCC and several unfavorable clinicopathological features especially Ki-67 labeling index. Furthermore, those ESCC patients with

FIGURE 5 Solute carrier family 34 member 2 (SLC34A2) promotes esophageal squamous cell carcinoma (ESCC) cell autophagy and proliferation by upregulating STX17. (a) Immunoprecipitation (IP) combined with Coomassie brilliant blue staining and mass spectrometry was used to identify the interacting proteins of SLC34A2. (b) The interaction between three top-ranking autophagy-related proteins and SLC34A2 was tested by IP and western blot (WB) in 293 T cells transfected with SLC34A2-HA or vector-HA. (c) Co-IP was used to verify the SLC34A2-STX17 interaction in ESCC cells. (d) The STX17 protein level was examined in SLC34A2-overexpressed/–silenced cells by WB. (e) WB was utilized to examine the levels of LC3B and P62 in SLC34A2-overexpressed ESCC cells under starvation conditions after silencing STX17. (f) The mRFP-GFP-LC3B reporter was performed to monitor the autophagic flux of SLC34A2-overexpressed ESCC cells with transient STX17 knockdown. Scale bar, 5 μ m. (g, h) Cell counting kit-8 (CCK-8) and 5-ethynyl-2'-deoxyuridine (EdU) assays were used to detect the proliferation ability of SLC34A2-overexpressed cells with transient STX17 knockdown. Scale bar, 20 μ m. (i) Five nude mice in each group were subcutaneously injected with KYSE520-SLC34A2 cells with STX17 knockdown, KYSE520-SLC34A2 cells and KYSE520 wild-type cells. The mean tumor volumes (cm^3) and weights (g) were measured 3 weeks later. The grayscale value of the target protein in the WB was quantified using ImageJ software and normalized to α -tubulin. ns, not significant; * $p < 0.05$; ** $p < 0.01$; *** $p < 0.001$.

upregulated SLC34A2 expression exhibited shorter OS and DFS. Functionally, it was found that ectopic overexpression or enforced knockdown of SLC34A2 in ESCC cells exerts promoting or inhibiting effects on cell proliferation *in vitro* and on tumor growth *in vivo*, respectively. These findings emphasize the oncogenic role of SCL34A2 in ESCC progression.

Emerging evidence demonstrates the close association between autophagy and tumor cell death as well as cell survival.^{29–31} In malignant cells, autophagy plays a dual role in promoting and inhibiting cancer growth and progression.^{32,33} Particularly, autophagy is enhanced to fulfill the high energetic demands of proliferating tumors during nutrient deprivation, thereby maintaining cell survival.^{34,35} Currently, autophagy inhibitors including CQ and HCQ are clinically explored and utilized to inhibit autophagy and tumor growth.^{36–39} However, clinical responses to autophagy-targeted drugs have varied widely.^{40–43} Thus, it is critical to investigate the role of autophagy in cancer for developing effective autophagy-targeted drugs. Previous studies have demonstrated the implication of phosphate cotransporter SLC34A2 in regulation of cell proliferation in various malignancies.^{10,11,28,44} It has recently been reported that the sodium-dependent phosphate cotransporter participated in autophagy regulation.⁴⁵ Notably, RNA-sequencing and GSEA showed revealed a positive correlation between high SLC34A2 expression and gene sets associated with autophagosome and autophagosome membrane in ESCC. Based on these findings, we further explore whether SLC34A2-mediated cell proliferation was dependent on autophagy. In this study, we observed that overexpression of SLC34A2 led to reduced p62 expression and upregulated LC3B expression. Moreover, overexpressing SLC34A2 resulted in an elevated number of autophagosomes and autolysosomes, indicating its ability to induce autophagy. Furthermore, activation of autophagy significantly attenuated the inhibitory effect on ESCC cell proliferation caused by SLC34A2 knockdown. Conversely, inhibition of autophagy alleviated pro-proliferative effect mediated by SLC34A2 overexpression in ESCC cells. These results underscore the role of SLC34A2 in promoting ESCC cell proliferation by inducing autophagy.

STX17 is an autophagosomal SNARE protein that mediates the fusion of autophagosome and lysosome membrane by interacting with SNAP-29 and VAMP8.^{21,46} STX17 is recruited to autophagosomes by directly binding to IRGM and mammalian Atg8s.⁴⁷ Deacetylation of STX17 facilitates the formation of the STX17-SNAP29-VAMP8 SNARE complex and enhances its interaction with HOPS.⁴⁸ ULK phosphorylation of STX17 facilitates its recruitment to autophagosomes and autophagosome maturation.⁴⁹ Furthermore, STX17 is phosphorylated at Ser-202 to participate in assembly of protein complexes and to induce autophagy.²² These findings highlight the crucial role played by STX17 in regulating autophagy. In this study, it was demonstrated that SLC34A2 bound to STX17 and regulated STX17 post-translationally. Moreover,

upregulation of STX17 expression by SLC34A2 promotes ESCC cell proliferation and autophagy. Recent studies have shown that STX17 was cleaved by a serine protease Lpg1137 in the ER-mitochondria contact site,^{50,51} indicating potential involvement of the proteasome pathway in regulating turnover of the STX17 protein. Our study further revealed that SLC34A2 interacted with STX17 to inhibit its ubiquitination and degradation. However, further investigation is needed to elucidate how exactly SLC34A2 exerts this inhibitory effect on degradation of STX17 protein. Additionally, silencing of STX17 was found to suppress the proliferation and autophagy of SLC34A2-overexpressed ESCC cells.

In summary, SLC34A2 is upregulated in ESCC and linked to adverse clinicopathological features and prognosis of ESCC patients. Furthermore, SLC34A2 binds to STX17 to induce autophagy by stabilizing STX17 protein, thereby promoting cell proliferation. These results provide compelling evidence for the oncogenic role and prognostic significance of SLC34A2 in ESCC.

AUTHOR CONTRIBUTIONS

Yi Xu: Data curation, investigation, methodology and writing—original draft. Shiyu Duan: Investigation and methodology. Wen Ye: Investigation, methodology, writing—review and editing. Zhousan Zheng: Methodology. Jiaying Zhang: Methodology. Ying Gao: Formal analysis, investigation, methodology, writing—review and editing. Sheng Ye: Funding acquisition, resources, supervision, writing—review and editing. All authors contributed to revision of the manuscript and read and approved the submitted version.

ACKNOWLEDGMENTS

We acknowledge the support of National Natural Science Foundation of China (no. 81772513) and the contributions of all the participators and authors of the study.

CONFLICT OF INTEREST STATEMENT

The authors do not have any competing interests to declare.

ORCID

Sheng Ye  <https://orcid.org/0000-0001-7857-9794>

REFERENCES

1. Sung H, Ferlay J, Siegel RL, Laversanne M, Soerjomataram I, Jemal A, et al. Global cancer statistics 2020: GLOBOCAN estimates of incidence and mortality worldwide for 36 cancers in 185 countries. *CA Cancer J Clin.* 2021;71(3):209–49.
2. Napier KJ, Scheerer M, Misra S. Esophageal cancer: a review of epidemiology, pathogenesis, staging workup and treatment modalities. *World J Gastrointest Oncol.* 2014;6(5):112–20.
3. de la Horra C, Hernando N, Lambert G, Forster I, Biber J, Murer H. Molecular determinants of pH sensitivity of the type IIa Na/P (i) cotransporter. *J Biol Chem.* 2000;275(9):6284–7.
4. Xu H, Bai L, Collins JF, Ghishan FK. Molecular cloning, functional characterization, tissue distribution, and chromosomal localization of a human, small intestinal sodium-phosphate (Na⁺-pi) transporter (SLC34A2). *Genomics.* 1999;62(2):281–4.

5. Hernando N, Gagnon K, Lederer E. Phosphate transport in epithelial and nonepithelial tissue. *Physiol Rev.* 2021;101(1):1–35.
6. Karim-Jimenez Z, Hernando N, Biber J, Murer H. Requirement of a leucine residue for (apical) membrane expression of type IIb NaPi cotransporters. *Proc Natl Acad Sci U S A.* 2000;97(6):2916–21.
7. Vlasenkova R, Nurgalieva A, Akberova N, Bogdanov M, Kiyamova R. Characterization of SLC34A2 as a potential prognostic marker of oncological diseases. *Biomolecules.* 2021;11(12). <https://doi.org/10.3390/biom11121878>
8. Liu L, Yang Y, Zhou X, Yan X, Wu Z. Solute carrier family 34 member 2 overexpression contributes to tumor growth and poor patient survival in colorectal cancer. *Biomed Pharmacother.* 2018;99:645–54.
9. Li Y, Chen X, Lu H. Knockdown of SLC34A2 inhibits hepatocellular carcinoma cell proliferation and invasion. *Oncol Res.* 2016;24(6):511–9.
10. Wang Y, Yang W, Pu Q, Yang Y, Ye S, Ma Q, et al. The effects and mechanisms of SLC34A2 in tumorigenesis and progression of human non-small cell lung cancer. *J Biomed Sci.* 2015;22(1):52.
11. He J, Zhou M, Li X, Gu S, Cao Y, Xing T, et al. SLC34A2 simultaneously promotes papillary thyroid carcinoma growth and invasion through distinct mechanisms. *Oncogene.* 2020;39(13):2658–75.
12. Lee J, Lee SE, Kang SY, do IG, Lee S, Ha SY, et al. Identification of ROS1 rearrangement in gastric adenocarcinoma. *Cancer-Am Cancer SOC.* 2013;119(9):1627–35.
13. Davies KD, Le AT, Theodoro MF, et al. Identifying and targeting ROS1 gene fusions in non-small cell lung cancer. *Clin Cancer Res.* 2012;18(17):4570–9.
14. Marshall RS, Vierstra RD. Autophagy: the master of bulk and selective recycling. *Annu Rev Plant Biol.* 2018;69:173–208.
15. Levine B, Kroemer G. Biological functions of autophagy genes: a disease perspective. *Cell.* 2019;176(1–2):11–42.
16. Assi M, Kimmelman AC. Impact of context-dependent autophagy states on tumor progression. *Nat. Cancer.* 2023;4:596–607.
17. Li X, He S, Ma B. Autophagy and autophagy-related proteins in cancer. *Mol Cancer.* 2020;19(1):12.
18. Amaravadi RK, Kimmelman AC, Debnath J. Targeting autophagy in cancer: recent advances and future directions. *Cancer Discov.* 2019;9(9):1167–81.
19. Eisenberg-Lerner A, Kimchi A. The paradox of autophagy and its implication in cancer etiology and therapy. *Apoptosis.* 2009;14(4):376–91.
20. Takats S, Nagy P, Varga A, et al. Autophagosomal Syntaxin17-dependent lysosomal degradation maintains neuronal function in drosophila. *J Cell Biol.* 2013;201(4):531–9.
21. Itakura E, Kishi-Itakura C, Mizushima N. The hairpin-type tail-anchored SNARE syntaxin 17 targets to autophagosomes for fusion with endosomes/lysosomes. *Cell.* 2012;151(6):1256–69.
22. Kumar S, Gu Y, Abudu YP, Bruun JA, Jain A, Farzam F, et al. Phosphorylation of Syntaxin 17 by TBK1 controls autophagy initiation. *Dev Cell.* 2019;49(1):130–44.
23. Matyskiela ME, Lu G, Ito T, Pagarigan B, Lu CC, Miller K, et al. A novel cereblon modulator recruits GSP1 to the CRL4(CRBN) ubiquitin ligase. *Nature.* 2016;535(7611):252–7.
24. Wu J, Gao F, Xu T, Li J, Hu Z, Wang C, et al. CLDN1 induces autophagy to promote proliferation and metastasis of esophageal squamous carcinoma through AMPK/STAT1/ULK1 signaling. *J Cell Physiol.* 2020;235(3):2245–59.
25. Li Y, Chen H, Yang Q, Wan L, Zhao J, Wu Y, et al. Increased Drp1 promotes autophagy and ESCC progression by mtDNA stress mediated cGAS-STING pathway. *J Exp Clin Cancer Res.* 2022;41(1):76.
26. Zhao Y, Zhu Z, Shi S, Wang J, Li N. Long non-coding RNA MEG3 regulates migration and invasion of lung cancer stem cells via miR-650/SLC34A2 axis. *Biomed Pharmacother.* 2019;120:109457.
27. Zhang L, Guo X, Zhang L, Yang F, Qin L, Zhang D, et al. SLC34A2 regulates miR-25-Gsk3beta signaling pathway to affect tumor progression in gastric cancer stem cell-like cells. *Mol Carcinog.* 2018;57(3):440–50.
28. Bao Z, Chen L, Guo S. Knockdown of SLC34A2 inhibits cell proliferation, metastasis, and elevates chemosensitivity in glioma. *J Cell Biochem.* 2019;120(6):10205–14.
29. Ronan B, Flamand O, Vescovi L, Dureuil C, Durand L, Fassy F, et al. A highly potent and selective Vps34 inhibitor alters vesicle trafficking and autophagy. *Nat Chem Biol.* 2014;10(12):1013–9.
30. Egan DF, Chun MG, Vamos M, et al. Small molecule inhibition of the autophagy kinase ULK1 and identification of ULK1 substrates. *Mol Cell.* 2015;59(2):285–97.
31. Debnath J, Gammoh N, Ryan KM. Autophagy and autophagy-related pathways in cancer. *Nat Rev Mol Cell Biol.* 2023;24(8):560–75.
32. Mizushima N. Autophagy: process and function. *Genes Dev.* 2007;21(22):2861–73.
33. Mizushima N, Yoshimori T, Ohsumi Y. The role of Atg proteins in autophagosome formation. *Annu Rev Cell Dev Biol.* 2011;27:107–32.
34. Rao S, Yang H, Penninger JM, Kroemer G. Autophagy in non-small cell lung carcinogenesis: a positive regulator of antitumor immunosurveillance. *Autophagy.* 2014;10(3):529–31.
35. Ma Y, Galluzzi L, Zitvogel L, Kroemer G. Autophagy and cellular immune responses. *Immunity.* 2013;39(2):211–27.
36. Rojas-Puentes LL, Gonzalez-Pinedo M, Crismatt A, Ortega-Gomez A, Gamboa-Vignolle C, Nuñez-Gomez R, et al. Phase II randomized, double-blind, placebo-controlled study of whole-brain irradiation with concomitant chloroquine for brain metastases. *Radiat Oncol.* 2013;8:209.
37. Barnard RA, Wittenburg LA, Amaravadi RK, Gustafson DL, Thorburn A, Thamm DH. Phase I clinical trial and pharmacodynamic evaluation of combination hydroxychloroquine and doxorubicin treatment in pet dogs treated for spontaneously occurring lymphoma. *Autophagy.* 2014;10(8):1415–25.
38. Mahalingam D, Mita M, Sarantopoulos J, Wood L, Amaravadi RK, Davis LE, et al. Combined autophagy and HDAC inhibition: a phase I safety, tolerability, pharmacokinetic, and pharmacodynamic analysis of hydroxychloroquine in combination with the HDAC inhibitor vorinostat in patients with advanced solid tumors. *Autophagy.* 2014;10(8):1403–14.
39. Rangwala R, Leone R, Chang YC, Fecher LA, Schuchter LM, Kramer A, et al. Phase I trial of hydroxychloroquine with dose-intense temozolomide in patients with advanced solid tumors and melanoma. *Autophagy.* 2014;10(8):1369–79.
40. Sotelo J, Briceno E, Lopez-Gonzalez MA. Adding chloroquine to conventional treatment for glioblastoma multiforme: a randomized, double-blind, placebo-controlled trial. *Ann Intern Med.* 2006;144(5):337–43.
41. Rosenfeld MR, Ye X, Supko JG, Desideri S, Grossman SA, Brem S, et al. A phase I/II trial of hydroxychloroquine in conjunction with radiation therapy and concurrent and adjuvant temozolomide in patients with newly diagnosed glioblastoma multiforme. *Autophagy.* 2014;10(8):1359–68.
42. Wolpin BM, Rubinson DA, Wang X, Chan JA, Cleary JM, Enzinger PC, et al. Phase II and pharmacodynamic study of autophagy inhibition using hydroxychloroquine in patients with metastatic pancreatic adenocarcinoma. *Oncologist.* 2014;19(6):637–8.
43. Boone BA, Bahary N, Zureikat AH, Moser AJ, Normolle DP, Wu WC, et al. Safety and biologic response of pre-operative autophagy inhibition in combination with gemcitabine in patients with pancreatic adenocarcinoma. *Ann Surg Oncol.* 2015;22(13):4402–10.
44. Ye W, Chen C, Gao Y, Zheng ZS, Xu Y, Yun M, et al. Overexpression of SLC34A2 is an independent prognostic indicator in bladder cancer and its depletion suppresses tumor growth via decreasing c-Myc expression and transcriptional activity. *Cell Death Dis.* 2017;8(2):e2581.
45. Dai XY, Zhao MM, Cai Y, Guan QC, Zhao Y, Guan Y, et al. Phosphate-induced autophagy counteracts vascular calcification by reducing matrix vesicle release. *Kidney Int.* 2013;83(6):1042–51.
46. Diao J, Liu R, Rong Y, Zhao M, Zhang J, Lai Y, et al. ATG14 promotes membrane tethering and fusion of autophagosomes to endolysosomes. *Nature.* 2015;520(7548):563–6.

47. Kumar S, Jain A, Farzam F, Jia J, Gu Y, Choi SW, et al. Mechanism of Stx17 recruitment to autophagosomes via IRGM and mammalian Atg8 proteins. *J Cell Biol.* 2018;217(3):997–1013.
48. Shen Q, Shi Y, Liu J, Su H, Huang J, Zhang Y, et al. Acetylation of STX17 (syntaxin 17) controls autophagosome maturation. *Autophagy.* 2021;17(5):1157–69.
49. Wang Y, Que H, Li C, et al. ULK phosphorylation of STX17 controls autophagosome maturation via FLNA. *J Cell Biol.* 2023;222(8). <https://doi.org/10.1083/jcb.202211025>
50. Arasaki K, Mikami Y, Shames SR, Inoue H, Wakana Y, Tagaya M. Legionella effector Lpg1137 shuts down ER-mitochondria communication through cleavage of syntaxin 17. *Nat Commun.* 2017;8:15406.
51. Arasaki K, Tagaya M. Legionella blocks autophagy by cleaving STX17 (syntaxin 17). *Autophagy.* 2017;13(11):2008–9.

SUPPORTING INFORMATION

Additional supporting information can be found online in the Supporting Information section at the end of this article.

How to cite this article: Xu Y, Duan S, Ye W, Zheng Z, Zhang J, Gao Y, et al. SLC34A2 promotes cell proliferation by activating STX17-mediated autophagy in esophageal squamous cell carcinoma. *Thorac Cancer.* 2024;15(17):1369–84. <https://doi.org/10.1111/1759-7714.15314>